a reprint from Applied Optics

Time-resolved emission studies of ArF-laser-produced microplasmas

Josef B. Simeonsson and Andrzej W. Miziolek

ArF-laser-produced microplasmas in CO, CO_2, methanol, and chloroform are studied by time-resolved emission measurements of the plasma decay. Electron densities are deduced from Stark broadening of the line profiles of atomic H, C, O, and Cl. Plasma ionization and excitation temperatures are determined from measurements of relative populations of ionic and neutral species produced in the plasmas. A discussion of the thermodynamic equilibrium status of ArF-laser microplasmas is presented. In general, the ArF-laser-produced microplasma environment is found to be similar in all the gases studied, in terms of both temperature (15,000–20,000 K) and electron density (10^{17} cm^{-3}–10^{18} cm^{-3}), despite the considerable differences observed in the breakdown thresholds and relative energies deposited in the various gases.

Introduction

Laser-produced plasmas have been widely used as vaporization, atomization, or excitation sources for chemical analysis of solid, liquid, and gas phase samples.[1–14] Since these plasmas are optically coupled, they are well defined spatially, easy to translate spatially, and free from electrodes and electrode contamination. For these reasons, they are well suited for field application and readily adaptable for applications to hostile or remote environments.[3,8,9,11] In most previous analytical applications, laser-produced plasms have been generated by using visible and IR wavelength lasers. Recently there have been a number of applications that use UV laser-produced plasmas. While the majority of analytical applications have been toward the analysis of solids, laser-produced plasmas have also been used effectively in the chemical analysis of gases.[9–14]

The mechanism for laser-induced breakdown of gases by using high peak-power pulsed lasers is generally believed to involve three consecutive processes: multiphoton absorption, which leads to ionization and the establishment of an initial electron density; continuum absorption of the laser radiation by the free electrons (inverse brehmsstrahlung); and electron collisions that lead to further ionization of the gas, which increases the electron density and ultimately leads to cascade ionization and heating (breakdown) of the gas.[15] The initial photoionization step typically occurs by way of nonresonant absorption and thus requires the use of lasers that can provide high peak intensities (10–100 GW/cm^2). The intensity threshold for optical breakdown is determined primarily by the efficiency of the multiphoton-ionization process. If the multiphoton absorption step proceeds by way of one or more resonant absorptions, the threshold for breakdown is reduced significantly.[15]

Recently a novel application of laser-produced plasmas for chemical analysis was reported.[12,13] A laser microplasma gas chromatography detector (LM-GCD) that uses focused radiation at 193 nm of an ArF excimer laser to create a breakdown microplasma in the effluent of a gas chromatograph column was developed. Microplasma formation is believed to be enhanced by a resonant absorption of 193-nm radiation by C atoms ($2p3s\ ^1P_1 \leftarrow 2p^2\ ^1D_2$) that are produced from the photodissociation of C that contains analyte molecules in the effluent.[16–18] It has been observed that microplasmas formed in this manner can be produced with unusually low laser pulse energies (< 1 mJ) and with low-number densities of C-bearing molecules. The LM-GCD has a high degree of chemical selectivity as a result of the characteristic atomic and molecular emissions of species in the plasma. The LM-GCD also has virtual universal responsivity to any C-containing compounds, including CO, CO_2, and halogenated species, which are difficult to detect with a conventional flame ionization

The authors are with the U.S. Army Ballistic Research Laboratory, SLCBR-IB-I, Aberdeen Proving Ground, Maryland 21005-5066.

Received 26 June 1992.
0003-6935/93/060939-09$05.00/0.
© 1993 Optical Society of America.

detector (FID). However, the plasma environment of the LM-GCD has not yet been studied in any detail or characterized in terms of its basic parameters, such as temperature and density. It is important to evaluate these physical characteristics in order to understand this phenomenon better and to expand the future applications of ArF-laser-produced microplasmas.

The purpose of this paper is to determine the physical characteristics of ArF-laser-produced microplasmas in different gases that consist of C-bearing molecules. Temperature and electron density information have been obtained from the spectroscopic measurement of the elemental emissions of H, C, O, and Cl atoms and ions. All the measurements reported are line-of-sight emissions and represent population average values. No attempt has been made at spatially resolving the measurements within different parts of the plasma. The methods used to determine the plasma temperatures assume a state of (local) thermodynamic equilibrium, and, thus, an evaluation of the validity of this assumption has been carried out as well.

Experimental

The instrumentation used in ArF-laser-induced microplasma studies is similar to that used in previous studies of the LM-GCD.[12,13] An ArF laser (Lambda Physik, LPX 105e) that was used to produce the laser breakdown microplasmas provided approximately 10-mJ pulses at 193 nm in pulses lasting 10 ns. To ensure good focusing of the laser radiation, it was necessary to use unstable resonator optics in the excimer laser cavity. The radiation was transmitted by a dielectric-coated mirror and a lens with a focal length of 25 cm. A calorimeter (38-1UV5, Scientech Inc.) was used to monitor the transmitted laser power and was placed behind the focal point of the focusing lens. The excimer laser output was adjusted by variation of the discharge voltage in the cavity, by attenuating the beam with dielectric-coated beam splitters, or by a combination of both. At the focal point, the laser beam was positioned 1 mm above the output of a Cu tube (1.4-mm i.d.) through which the plasma gas flowed (150 cm^3/min). Linear flow velocities at the tube orifice were 150 cm/s. The flow tube was positioned concentrically inside another tube (9-mm i.d.) through which He flowed as a sheath gas (1 L/min.). He sheath gas was used to isolate the sample gas tube from the laboratory atmosphere, and was also used to prevent breakdown from occurring except when a C-containing gas was present. It was confirmed that breakdown occurred only when a C species was flowed from the center tube.

The plasma emission was collected perpendicular to the direction of the laser beam by a quartz lens and imaged with unit magnification onto the slit of a 0.5-m spectrometer (SPEX-500, SPEX Industries) equipped with either a UV- or IR-sensitive photomultiplier tube (PMT) (Thorn EMI models 9628Q and 9658R, respectively). The voltage output of the PMT was processed by a boxcar–gated integrator (Stanford Research Systems) and stored on a personal computer for data analysis. Plasma emissions were collected by scanning the spectrometer over the wavelengths of interest at a constant time delay with respect to the incident laser pulse. Time resolution of the plasma emission was obtained by adjusting the boxcar delay in 100-ns steps in which time zero coincided with the laser pulse.

The gases in which the plasmas were formed were obtained from Matheson (CO, CO_2; >99.5% purity) or were introduced at their room-temperature partial pressures as vapors in flowing He (methanol, chloroform; Fisher Scientific). The spectroscopic temperature measurements required that the detector response be calibrated as a function of wavelength. We performed this by using a W filament standards lamp (EPT-1293, Eppley Laboratory Inc.). When measuring emissions above 450 nm it was also necessary to place a long-pass filter (GG-455, Schott Filter Glass Inc.) in front of the entrance slit of the spectrometer to remove the second-order transmissions of shorter wavelengths. To correct for instrumental broadening in the measured linewidths, we determined the linewidth of the spectrometer by using a low-pressure Hg light source at 253.6 nm.

Results and Discussion

The gross spectral features of ArF-laser-induced microplasmas have been reported previously.[12] In general, the spectra are dominated by emissions of C, O, and H neutrals and include emissions of small diatomic species such as CH, C_2, and OH. The plasma emission in this paper typically lasted ~1–2 μs, with a strong continuum occurring early in the plasma lifetime (t < 0.4 μs) and accompanied by ionic emissions. The remainder of the plasma decay was due to the much stronger neutral and diatomic emissions.

Initially the ArF-laser microplasmas were characterized in terms of their breakdown thresholds and relative absorption of the laser radiation. The intensity breakdown threshold I_{bd} (GW/cm^2) is the minimum peak laser intensity required for causing breakdown in the gas. The energy deposited in the microplasma E_{dep} was measured for 10-mJ incident pulse energies and was taken as the difference in the incident and the transmitted laser energies. Scattering of the laser light by the microplasma was checked for and was assumed to be minimal in the forward and reverse directions.

I_{bd} and E_{dep} for CO, CO_2, methanol, and chloroform are reported in Table 1 for the purpose of comparison of the different gases. The differences in the values of I_{bd} and E_{dep} are most likely due to the differences in the chemical structure, bond strengths, and ionization potentials of the various compounds. The compounds that photodissociate most readily will also form ions and electrons first. For compounds that form electrons early during the laser pulse, there is more laser energy available to be absorbed by the microplasma. It is intuitive, then, that a lower value of I_{bd} will result in a higher E_{dep}.

Table 1. Intensity Thresholds for Breakdown and Deposited Energies at 193 nm

(P_{total} = 1 atm)	I_{bd} (GW/cm^2)[a]	E_{DEP} (mJ)[b]
CH_3OH/He	10 ± 2.4	3.5
CO	24 ± 2.4	4
CO_2	68 ± 15	2.5
$CHCl_3$/He	6 ± 1.4	6.5

[a] I_{bd} is the breakdown intensity at the laser focus; pulse duration is 10^{-8} s; the area of focal spot is estimated to be 5×10^{-6} cm^{-2}.
[b] E_{dep} corresponds to the amount of energy absorbed by the microplasma for 10-mJ incident laser pulse energy.

It is important to note that the concentrations of the various gases are not the same in this paper. Whereas CO and CO_2 are at 1 atm, the partial pressures of methanol and chloroform are roughly 0.15 and 0.33 atm, respectively, at room temperature. No attempt has been made to study the concentration dependence of I_{bd} or E_{dep}. It is anticipated that the values of I_{bd} will decrease and E_{dep} will increase for both methanol and chloroform as their concentrations are increased.

It is also interesting to note the comparison of the intensity threshold for the ArF-laser-induced microplasmas in CO_2 with those that use different wavelength lasers. At 690 nm (ruby excitation) I_{bd} is 300 GW/cm^2, and at 1064 nm (Nd:YAG excitation) I_{bd} is 110 GW/cm^2 (see Ref. 15). However, at 193 nm it is significantly lower (68 GW/cm^2). The low threshold for CO_2 (and CO, methanol, and chloroform as well) is presumably at least partially due to the resonance absorption step of the C atoms, which greatly enhances the initial ionization rate and thus lowers the laser intensity that is necessary to cause breakdown.[16–18]

Plasma Density

Electron density is an important parameter that is used to describe a plasma environment and is crucial for establishing its equilibrium. The electron density is usually measured from the Stark broadening of emission lines of major species in the plasma.[19] In low-temperature plasmas of high density, the dominant broadening mechanism of the line profile is Stark broadening (as opposed to Doppler broadening). Since Stark broadening is relatively independent of the temperature, the electron density can be calculated with good accuracy even when the temperature is not well known. The technique of determining the electron density from the linewidths of H atom emissions is especially well known.[20] H atomic emissions offer a convenient means of measuring the plasma electron density because they undergo a linear Stark effect, that is, the broadening is directly proportional to the magnitude of the electric field, which is a function of the electron density. The Stark-broadened profiles of H are usually wide (> 1 nm) and easy to measure with a typical laboratory spectrometer.

In relatively low-density plasmas ($N_e < 10^{16}$ cm^{-3}) the electron density is measured from the Stark profile of the beta emission line of the H Balmer series (486.1 nm). However, in higher-density plasmas, this line becomes too broad to be measured accurately and alternative lines must be used. The electron density in laser-generated plasmas has been reported previously to be of the order of 10^{16}–10^{18} cm^{-3} (see Refs. 9 and 21). The broadening of the H alpha line of the Balmer series at 656.2 nm can be measured accurately in the range 10^{15}–10^{18} cm^{-3} and is well suited for the range of electron densities expected in a laser-produced plasma.[22] Spectral scans that illustrate the Stark broadening of the H alpha emission line at two delay times in the decay of microplasmas formed in methanol are shown in Fig. 1. The Stark broadening of the profile is clearly seen and is more pronounced early in the decay when the electron density is relatively high.

In CO and CO_2, however, one must use other species to determine the electron density. At sufficiently high electron densities, the less-pronounced Stark broadening (quadratic Stark effect[19,20]) C, O, and Cl emissions are measurable and can be used to determine the density. In this paper, the electron density was determined from the Stark broadening of C atoms at 247.9 nm in all the gases, from O atoms at 845 nm in CO, CO_2, and methanol, from H atoms at 656.2 nm in methanol and chloroform, and from Cl atoms at 725.6 nm in chloroform. The measured linewidths (FWHM) were corrected for Doppler and instrumental broadening and used to calculate the electron density according to methods developed previously by Griem.[20] In Fig. 2, the average electron density, as determined from the Stark broadening of these species, is plotted for each of the gases as a function of the decay time of the ArF-laser-produced microplasmas. It is observed that the relative mag-

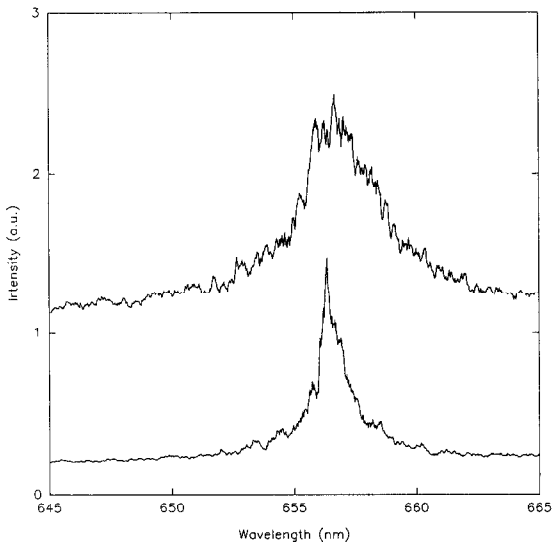

Fig. 1. Spectra showing the Stark-broadened profiles of the H Balmer alpha emission at 656.2 nm at times 0.3 μs (upper trace) and 0.9 μs (lower trace) after the laser pulse. a.u., arbitrary units.

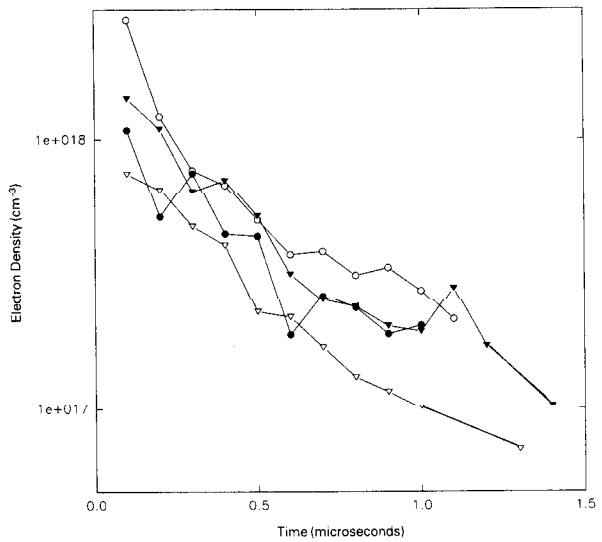

Fig. 2. Plot of microplasma electron densities as a function of time for CO (open circles), CO_2 (filled circles), methanol (open inverted triangles) and chloroform (filled inverted triangles).

nitudes and temporal profiles of the electron density in the different plasma environments are similar.

In general terms, the electron density follows the same trend in all the microplasma environments. The electron density is at a maximum at the earliest times and is of the order of 10^{18} cm^{-3} or greater. The density decays steadily to $\sim 10^{17}$ cm^{-3} or less within 1 μs. The maximum electron density measured in these studies is similar to that reported by others in studies of laser-produced plasmas in the gas phase.[9,15,21] The high electron density suggests that the microplasmas are likely to be at or near a state of local thermodynamic equilibrium (LTE). The assumption of LTE is important for the determination of plasma temperatures from spectroscopic measurements that require the use of Saha and Boltzmann equilibrium relations. A further discussion of the LTE considerations follows below.

Excitation Temperature

The excitation temperature of ArF-laser-produced plasmas has been measured by using the ratios of spectrally integrated emission intensities of emission lines of O and Cl neutrals formed as either initial photodissociation products or subsequent high-temperature fragments of vapors in which the microplasma is formed. The integrated emission intensities can be correlated to a temperature through the familiar Boltzmann relation. For CO, CO_2, and methanol, O emissions at 777 nm [$2p^3 3p\ ^5P$ (86 629 cm^{-1}) ← $2p^3 s\ ^5S$ (73 768 cm^{-1})] and 795 nm ($2p^3 3p'\ ^3F$ (113 719 cm^{-1}) ← $2p^3 3s'\ ^3D$ (101 143 cm^{-1})] were chosen because of their relative intensity and close spectral proximity that reduced inaccuracies that were due to changes in the spectral response of the detector. Cl neutral emissions at 725.6 nm [$3p^4 4p\ ^4S$ (85 731 cm^{-1}) ← $3p^4 4s\ ^4P$ (71 954 cm^{-1})] and 808.8 nm [$3p^4 4p'\ ^2D$ (96 480 cm^{-1}) ← $3p^4 4s\ ^2D$ (84 116 cm^{-1})] were chosen for chloroform. When evaluating plasma temperatures by this method, it is important to verify that the plasmas are not optically thick. This was done by checking the ratio of emission intensities of the three O emission lines at 777.196 nm, 777.418 nm, and 777.540, nm according to a procedure described previously by Radziemski et al.[9] The intensities were observed to be in a ratio that is consistent with the ratio of their statistical weights, which indicates that the plasma was not optically thick.

Figure 3 is a plot of the measured excitation (Boltzmann) temperature shown as a function of the ArF-laser-produced plasma lifetime with O and Cl as thermometric probes for microplasmas formed in CO, CO_2, methanol, and chloroform vapors. The same range (11,000–19,000 K) and slow decay behavior of the O atom temperatures have been observed previously in another study of laser breakdown plasmas formed in air.[21] The strong continuum background and broadening of the emission profiles prevented determinations of the Cl excitation temperature before times of 0.5 μs. It is noted that the O and Cl temperature appear to be quite close to each other, despite the differences in the plasma gases and the values of I_{bd} and E_{dep}.

Ionic Temperature

The ionic temperature of the ArF-laser-produced plasma has been measured from the integrated emission intensities of neutral C atoms measured at 247.9 nm [$2p3s\ ^1P_1$ (61 982 cm^{-1}) ← $2p^2\ ^1S_0$ (21 648 cm^{-1})] to that of singly ionized C atoms measured at 251.1 nm [$2p^3\ ^2D$ (150 465 cm^{-1}) ← $2s2p^2\ ^2P$ (110 652 cm^{-1})]. Figure 4 is a survey spectrum of the region showing the neutral and ionic emissions of C in a CO microplasma at a delay time of 0.3 μs. As in the case of the O excitation temperature, these two C emissions were

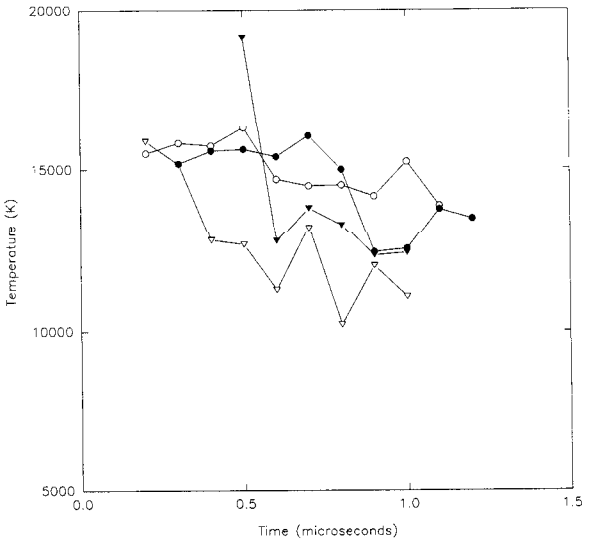

Fig. 3. Plot of the Boltzmann excitation temperatures as a function of time, with O as the thermometric probe species for CO (open circles), CO_2 (filled circles), and methanol (open inverted triangles), and with Cl as the thermometric probe for chloroform (filled inverted triangles).

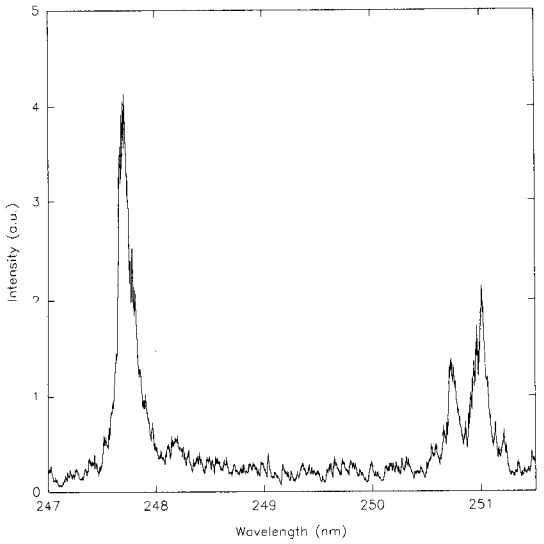

Fig. 4. Spectrum showing the relative intensity of C neutral and ion emissions at 247.9 nm and 251.1 nm, respectively, in CO microplasmas at 0.3 μs after the laser pulse.

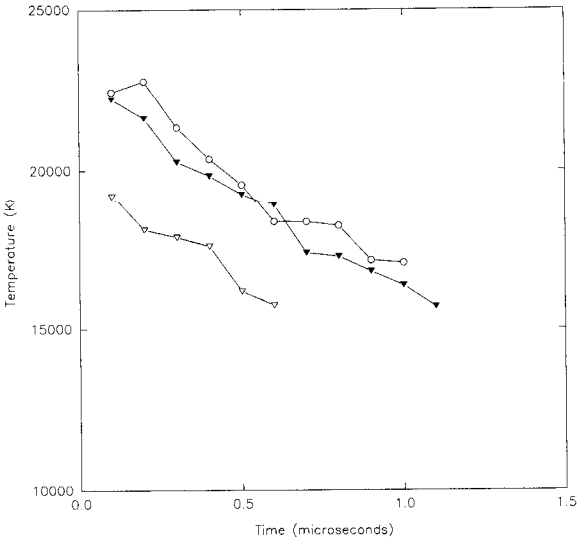

Fig. 5. Plot of the ionization temperatures as functions of time, with C as the thermometric probe species for CO (open circles), methanol (open inverted triangles), and chloroform (filled inverted trianges).

selected because of their relative intensity and close proximity spectrally, which minimizes error that is due to changes in the spectral response of the detection system. Using the Saha and Boltzmann relations along with knowledge of the electron density N_e, we find the ionic temperature from[23]

$$\frac{I_{\text{ion}}}{I_{\text{atom}}} = \frac{4.83 \times 10^{15}}{N_e}\left(\frac{gA}{\lambda}\right)_{\text{ion}}\left(\frac{\lambda}{gA}\right)_{\text{atom}} \times T_{\text{ion}}^{3/2}\exp\left[\frac{-(V^+ + E_{\text{ion}} - E_{\text{atom}})}{kT_{\text{ion}}}\right], \quad (1)$$

where I is the integrated emission intensity of the ion or atom (arbitrary units), N_e is the electron density (cm^{-3}), gA is the product of the statistical weight and Einstein coefficient for spontaneous emission of the upper level (s^{-1}), λ is the wavelength (nm), T_{ion} is the ion temperature (K), V^+ is the ion potential of the atom (J), E_{ion} is the excitation energy of the ion (J), E_{atom} is the excitation energy of the atom (J), and k is Boltzmann's constant (J/K). The temporal profile of the ionic temperature with C as the thermometric species in CO, methanol, and chloroform microplasmas is shown in Fig. 5. As noted above for O and Cl, there appears to be great similarity of the C ion temperatures in the three plasma environments.

While ionic C emissions were observed in all the gases, the ion emissions were accompanied by a strong continuum emission present early in the microplasma decay. Therefore, in the case of CO_2, in which the ionic emissions were not sufficiently strong, it was not possible to make a measurement of the ion temperature with a good signal-to-noise ratio. No O ion emissions were observed in any of the ArF-laser microplasmas. This is probably because the lowest states observable for O ions are greater than 24 eV above the ionic ground state and are relatively unpopulated.

In chloroform microplasmas, both neutral and singly charged ion Cl species were observed, which made it possible to use another species to measure the ion temperature. Ionic emissions were observed at 479.454 nm [$3p^3 4p\ ^5p$ (123 730 cm^{-1}) ← $3p^3 4s\ ^5S$ (107 879 cm^{-1})] and were used with the neutral line at 725.6 nm. Temperatures determined from these measurements are in excellent agreement with ion temperatures of C in chloroform. A summary of the measured temperatures (ion and excitation) and electron densities as a function of time for microplasmas formed in CO, CO_2, methanol, and chloroform are given in Tables 2, 3, 4, and 5, respectively.

It is interesting to note that, despite the considerable differences in the values of I_{bd} and E_{dep}, the various microplasmas are characterized by similar values of temperature and electron density. Intuitively, it might seem likely that a significantly higher E_{dep} would contribute to higher temperatures and densities in the microplasma. However, it is well known that, once breakdown occurs, the plasma

Table 2. Electron Density and Temperatures of CO Microplasmas

Time (μs)	N_e (10^{17} cm $^{-3}$)	T_{exc} (K)	T_{ion} (K)
0.1	27.5	—	22,500
0.2	12.1	15,500	22,800
0.3	7.69	15,800	21,300
0.4	6.77	15,700	20,400
0.5	4.99	16,300	19,600
0.6	3.74	14,700	18,400
0.7	3.84	14,900	18,400
0.8	3.14	14,500	18,200
0.9	3.35	14,200	17,200
1.0	2.75	15,200	17,100
1.1	0.82	13,900	

Table 3. Electron Density and Temperature of CO_2 Microplasmas

Time (μs)	N_e (10^{17} cm^{-3})	T_{exc} (K)	T_{ion} (K)
0.1	10.8	—	—
0.2	5.13	15,200	—
0.3	7.49	15,600	—
0.4	4.44	15,600	—
0.5	4.35	15,400	—
0.6	1.88	16,000	—
0.7	2.63	15,000	—
0.8	2.36	12,400	—
0.9	1.89	12,500	—
1.0	2.03	14,600	—
1.1	—	13,800	—
1.2	—	13,500	—

region becomes opaque to the laser radiation, and any additional laser energy only causes the microplasma to grow in size in the direction of the laser source.[9] At these power densities, optical breakdown effectively puts a limit on the amount of laser energy that can be supplied and, thus, on the level of excitation that can be achieved in the microplasma region. Therefore the similarity in the characteristic temperatures and densities of the ArF-laser-produced microplasmas is not surprising.

There are a number of factors that contribute to the uncertainty associated with the temperatures reported here. It is well known that the accuracy of these methods of temperature measurement are fundamentally limited by uncertainty in the oscillator strength or coefficients of spontaneous emission.[23] A list of the wavelengths, upper-state energies, and statistical weights and spontaneous emission coefficients (gA values) used in this paper along with the relative uncertainty in the gA values is given in Table 6. In the case of O, the oscillator strengths contribute approximately 25% uncertainty to the ratio of integrated intensities and in the case of C and Cl, they contribute approximately 50%. Uncertainty in the ratio of intensities, however, does not translate directly into a similar uncertainty in the temperature.

The uncertainty in the temperature determination by the two methods used in this study is given by

Table 4. Electron Density and Temperatures of CH_3OH Microplasmas

Time (μs)	N_e (10^{17} cm^{-3})	T_{exc} (K)	T_{ion} (K)
0.1	7.46	—	19,200
0.2	6.49	15,900	18,100
0.3	4.73	15,200	17,900
0.4	4.04	12,800	17,600
0.5	2.28	12,600	16,200
0.6	2.18	11,300	15,800
0.7	1.69	13,200	—
0.8	1.32	10,200	—
0.9	1.17	12,000	—
1.0	1.02	11,000	—
1.3	0.71	—	—

Table 5. Electron Density and Temperatures of $CHCl_3$ Microplasmas

Time (μs)	N_e (10^{17} cm^{-3})	T_{exc} (K)	T_{ion} (K)
0.1	14.1	—	22,200
0.2	10.9	—	21,600
0.3	6.42	—	20,300
0.4	7.04	—	19,800
0.5	5.15	19,100	19,500
0.6	3.17	12,800	19,100
0.7	2.53	13,800	17,300
0.8	2.38	13,300	17,000
0.9	2.02	12,300	16,800
1.0	1.93	12,400	16,300
1.1	2.18	—	15,800
1.2	1.71	—	—
1.4	1.04	—	—
1.6	0.58	—	—

Refs. 23 and 26:

$$\frac{\Delta T}{T} = \frac{kT}{\Delta E}\frac{\Delta R}{R}, \tag{2}$$

where T is the temperature (K), k is Boltzmann's constant (J/K), ΔE is the difference in energy of the two states observed (J), and R is the ratio of measured emission intensities. This equation is useful because it illustrates how errors or uncertainties in the experimental measurement are translated into uncertainty in the resulting temperature. The factor $kT/\Delta E$ scales the relative uncertainty in R into relative uncertainty in T. This factor can be viewed as the ratio of the thermal energy of the plasma (kT) to ΔE, which is the difference in energy of the two thermometric states observed. It is clear from Eq. (2) that large values of ΔE minimize the effect of uncertainty in R on the uncertainty in T.

In the cases of O and Cl excitation temperatures, ΔE and kT are of the same order and the degrees of uncertainty in R and T are also roughly the same. For example, in the case of O, ΔT is ~15% because of the oscillator strengths. For the Cl neutrals, $kT/\Delta E$ is approximately 1, and the uncertainty in the excitation temperature may be as high as 70% because of the oscillator strengths alone.

Table 6. Wavelengths, State Energies, and Transition Probabilities

Element	λ (nm)	E_u (cm^{-1})[a]	g_uA_{ul} (10^8 s^{-1})	Uncertainty (%)[b]
C (I)	247.856	61,982	1.02	>50 (Ref. 24)
C (II)[c]	251.1	150,465	9.7	>50 (Ref. 24)
O (I)[c]	777.34	86,629	5.1	<10% (Ref. 24)
O (I)[c]	794.93	113,719	7.83	<25 (Ref. 24)
Cl (I)	725.663	85,731	0.76	<50 (Ref. 25)
Cl (I)[c]	808.58	96,480	4.2	<50 (Ref. 25)
Cl (II)	479.454	128,730	8.26	<25 (Ref. 25)

[a] E_u is the energy of the upper state in cm^{-3}.
[b] Estimated uncertainty in g_uA_{ul} as reported in Refs. 24 and 25.
[c] Wavelengths and E_u are average values for the multiplets.

By comparison, in the ion temperature determinations ΔE is of the order of 15–20 eV (much larger than kT) and the uncertainty in T is much less than the uncertainty in R. The uncertainty in the temperatures of Cl and C should be of the order of 6% and 7%, respectively. The ion temperatures should be regarded as more reliable than the excitation temperatures. One would also expect better agreement and less scatter among the various ion temperature determinations, as has been observed experimentally (see Fig. 5).

Equilibrium Considerations

For the purposes of determining the plasma temperatures, it was necessary to assume that the ArF-laser-produced plasma reached a state of LTE soon after its formation. There are several reasons why LTE conditions are believed to exist. In an LTE plasma, it is necessary that the velocity distribution of the free electrons be Maxwellian. Griem has stated that in relatively dense, low-temperature plasmas ($N_e > 10^{16}$ cm^{-3}; $kT < 5$ eV), the electron velocity distribution is nearly always Maxwellian.[27] The ArF-laser microplasmas have electron densities ranging from 10^{16} to 10^{18} cm^{-3} and temperatures of ~1–2 eV, therefore one expects that the free-electron velocity distribution will be Maxwellian.

Furthermore, in an LTE plasma the collision excitation and de-excitation processes must dominate with respect to the radiative processes, which require a minimum electron density. The minimum electron density necessary for LTE between two states separated in energy by ΔE (eV) is a function of the temperature (K) and is given by the following expression[28]:

$$N_e \gg 1.6 \times 10^{18}\sqrt{T_e}(\Delta E)^3. \quad (3)$$

For $\Delta E < 5$ eV and a temperature of 15,000 K, N_e should be at least 10^{17} cm^{-3}. In the ArF-laser-induced microplasmas, N_e is in excess of 10^{17} cm^{-3} for ~1 μs. This suggests that LTE is likely to exist throughout the excited states of species in the microplasmas.

In the case of a transient plasma, such as a laser-produced microplasma, the magnitude of the electron density is significant because it indicates not only if LTE is possible but also how quickly a plasma will proceed toward LTE once it is formed. The time for establishing a kinetic equilibrium between electrons and heavier ions and neutrals is inversely proportional to the electron density and can be estimated from the following expression[23]:

$$t_{kin} \cong \left[7.5 \times 10^{-7}\left(\frac{X_H}{kT}\right)^{3/2} N_e\right]^{-1} \frac{nm}{n^+ m_e}, \quad (4)$$

where X_H is the ionization potential of hydrogen (J), n^+ is the number density of neutral or charged species (cm^{-3}), m is the atomic mass (g), and m_e is the electron mass (g). In a laser microplasma that is ionized approximately 10%, where $N_e = 10^{18}$ cm^{-3} and $kT_e = 1.5$ eV (initial conditions), $t_{kin} = 10$ ns for particles up to $m = 50$ amu. In the current studies, kinetic equilibrium should be established within ~10 ns of the termination of the laser pulse.

The time for the excited-state distributions of the different species to equilibrate (according to a Boltzmann distribution) is given by a similar expression.[23,27] For the same conditions as above, the relaxation time of the excited states to a Boltzmann-like distribution ranges from 0.5 to 50 ns for the elements H, C, O and Cl. These times are calculated for the largest energy separations possible, i.e., resonance transitions from the ground state to the first excited state, and represent the upper limit on the time for relaxation. Equilibration times for states that are closer (between two excited states) will be even less.

Experimental evidence also supports the assumption of LTE in the ArF-laser microplasmas. In prior studies of Nd:YAG- and CO_2-laser-induced plasmas formed in air and other gases, different groups have found evidence of LTE in the plasmas soon after their formation.[9,21,29] Radziemski *et al.* concluded from their studies that laser-induced air plasmas appear to be at or near a state of LTE at 1 μs after the laser pulse.[9] Theoretical studies of the temperature and electron density based on a model of an equilibrium CO_2 plasma at atmospheric pressure also support the assumption of LTE. The values predicted by the model are in good agreement (within approximately 10%) with values measured in this study for CO_2 microplasmas at 1 μs.[30]

An important requirement of LTE plasmas is close agreement of measurements of the different energy distributions, i.e., kinetic, ionization, and excitation (Boltzmann) temperatures. In this paper, it is possible to compare different temperatures in CO, methanol, and chloroform microplasmas. Temporal profile plots of the ion and excitation temperatures measured for chloroform and CO, respectively, are shown in Figs. 6 and 7. Figure 6 shows that there is excellent agreement between the ion temperature measurements for C and Cl species in the chloroform microplasmas, which supports the argument that ion temperature measurements are less susceptible to both theoretical and experimental uncertainties than excitation temperatures. However, differences in the ion and excitation temperatures are seen in both figures. The ion temperatures are initially higher but then decay toward the values of the excitation temperatures, which remain fairly stable throughout the plasma decay (see Figs. 6 and 7). By extrapolation to times beyond 1 μs, it appears that the ion and excitation temperatures converge. Because of low emission intensities and poor signal-to-noise ratios, temperature measurements beyond 1 μs were not possible and such a convergence could not be verified.

As mentioned above the temperatures being reported include a not insignificant degree of uncertainty. The uncertainty makes it difficult to compare the C, O, and Cl temperatures directly and thus

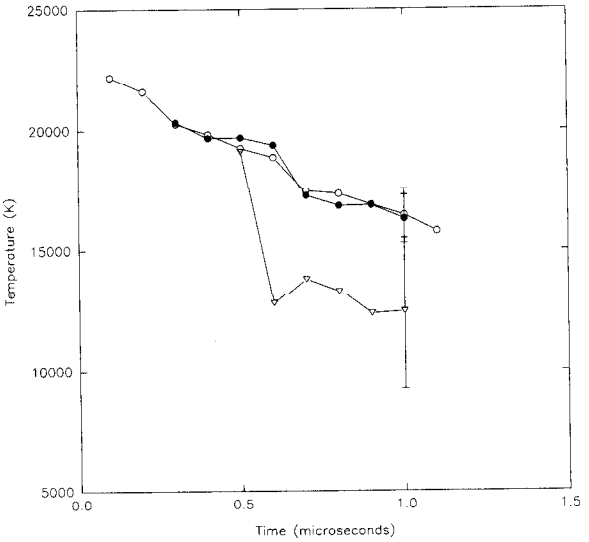

Fig. 6. Plot of the ionization temperatures of C (open circles) and Cl (filled circles) and the excitation temperature of chlorine (open inverted triangles) in chloroform microplasmas as a function of time.

to determine if they are in agreement. Nonetheless, if ΔT is estimated to be 7% for the C temperatures and 15% for the O temperatures, then the ion and excitation temperatures are well within theoretical uncertainty by 1 μs for CO. Similarly for chloroform, if the uncertainty in the excitation temperature of Cl is conservatively estimated to be 25% and the uncertainty of the ion temperature of Cl is 6%, then the C and Cl ion and excitation temperatures are also within theoretical uncertainty by 1 μs. A more definitive demonstration of temperature agreement for these species would require better knowledge of the oscillator strengths or careful observation of several other states and (weaker) transitions.

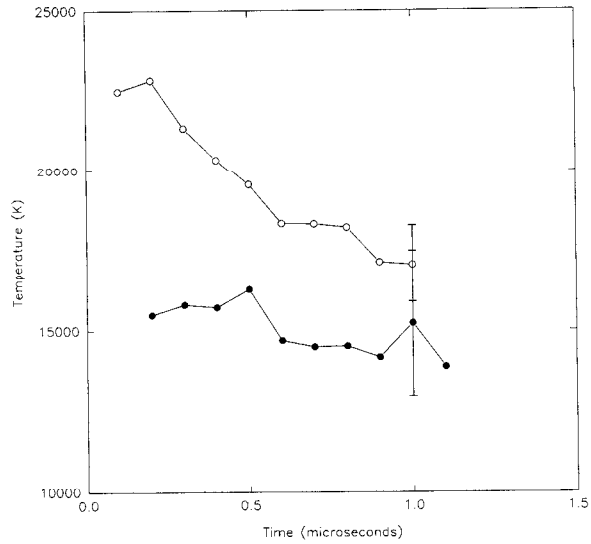

Fig. 7. Plot of the ionization temperature of C (open circles) and the excitation temperature of oxygen (filled circles) in CO microplasmas as a function of time.

The accuracy of Boltzmann-type temperature measurements can often be improved by preparing a Boltzmann plot of the populations of several states as a function of the corresponding state energies. This is difficult to accomplish with elements such as C, O, and Cl, for which the number of accessible states and transitions are limited. Instead, it would be preferable to seed a thermometric probe species that has numerous observable states into the microplasma environment. If possible, the use of multiple probe species would also improve the confidence of the overall temperature determination.

Conclusions

Time-resolved emission spectroscopy has been used to study ArF-laser-produced microplasmas formed in CO, CO_2, methanol, and chloroform. Unlike most laser-produced plasmas, ArF-laser-produced microplasmas formed in C-bearing gases can be generated with relatively low pulse energies and laser intensities. However, the characteristic temperature and density of the microplasmas have shown great similarities in different gases and are consistent with the results of plasma studies that use relatively high-power lasers in air and diatomic gases. These results suggest that despite significant differences in chemical structures, which are evidenced by the differences in the breakdown thresholds and deposited energies of the various gases, the microplasma environments are highly similar following breakdown for all the compounds studied. The ArF-laser-produced microplasma environment is believed to be in a state of LTE soon after its formation. The high electron density that is produced initially in the microplasma promotes rapid equilibration and efficient collisional coupling of the excited states. LTE is evidenced by the agreement of the CO_2 temperature and densities measured experimentally in this study with that predicted by an equilibrium model. LTE is also suggested by the agreement of the ion and excitation temperatures in three of the plasma environments. The use of a seeded thermometric species to probe the microplasma environment will improve the accuracy of future temperature determinations. Studies in this direction are currently in progress.

The authors thank Brad E. Forch for critical reading of the manuscript and helpful discussions. Partial support from U.S. Air Force Office of Scientific Research contract MIPR 91-0004 and support for equipment from the Productivity Investment Funding program administered by David Ellis are acknowledged. J. B. Simeonsson gratefully acknowledges support from the Ballistic Research Laboratory through the National Research Council Postdoctoral Associateship Program.

References

1. K. Neimax and W. Sdorra, "Optical emission spectrometry and laser-induced flourescence of laser produced plasmas," Appl. Opt. **29**, 5000–5006 (1990).
2. A. Quentmeier, W. Sdorra, and K. Neimax, "Internal standardization in laser induced fluorescence spectrometry of microplas-

mas produced by laser ablation of solid samples," Spectrochim. Acta **45B,** 537–546 (1990).
3. D. A. Cremers, "The analysis of metals at a distance using laser-induced breakdown spectroscopy," Appl. Spectrosc. **41,** 572–579 (1987).
4. K. J. Grant and G. L. Paul, "Electron temperature and density profiles of excimer laser-induced plasmas," Appl. Spectrosc. **44,** 1349–1354 (1990).
5. V. Majidi, J. T. Rae, and J. Ratliff, "Determination of trace metals using an electrothermal atomizer by laser-induced plasma atomic emission spectrometry," Anal. Chem. **63.** 1600–1602 (1991).
6. L. Nanai and I. Hevesi, "Time-resolved spectral investigations of laser light induced microplasma," Spectrochim. Acta **48A,** 19–24 (1992).
7. D. A. Cremers, L. J. Radziemski, and T. R. Loree, "Spectrochemical analysis of liquids using the laser spark," Appl. Spectrosc. **38,** 721–729 (1984).
8. J. R. Wachter and D. A. Cremers, "Determination of uranium in solution using laser-induced breakdown spectrometry," Appl. Spectrosc. **41,** 1042–1048 (1987).
9. L. J. Radziemski, T. R. Loree, D. A. Cremers, and N. M. Hoffmann, "Time-resolved laser-induced breakdown spectrometry of aerosols," Anal. Chem. **55,** 1246–1252 (1983).
10. D. A. Cremers and L. J. Radziemski, "Detection of chlorine and fluorine in air by laser-induced breakdown spectrometry," Anal. Chem. **55,** 1252–1256 (1983).
11. M. Casini, M. A. Harith, V. Palleschi, A. Salvetti, D. P. Singh and M. Vaselli, "Time-resolved LIBS experiment for quantitative determination of pollutant concentrations in air," Laser Part. Beams **9,** 633–639 (1991).
12. R. J. Locke, J. B. Morris, B. E. Forch, and A. W. Miziolek, "Ultraviolet laser microplasma-gas chromatography detector: detection of species-specific fragment emission," Appl. Opt. **29,** 4987–4992 (1990).
13. J. B. Morris, B. E. Forch, and A. W. Miziolek, "A novel detector for gas chromatography based on UV laser-produced microplasmas," Appl. Spectrosc. **44,** 1040–1043 (1990).
14. K. C. Ng, N. L. Ayala, J. B. Simeonsson, and J. D. Winefordner, "Laser-induced plasma atomic emission spectrometry in liquid aerosols," Anal. Chim. Acta (to be published).
15. D. C. Smith and R. G. Meyerand, Jr., "Laser radiation induced gas breakdown," in *Principles of Laser Plasmas,* G. Bekefi, ed. (Wiley, New York, 1976), pp. 458–478.
16. R. C. Sausa, A. J. Alfano and A. W. Miziolek, "Efficient ArF laser production and detection of carbon atoms from simple hydrocarbons," Appl. Opt. **26,** 3588–3593 (1987).
17. H. F. Dobele and B. Ruckle, "Detection of carbon impurities in plasmas by atomic fluorescence spectroscopy," J. Nucl. Mater. **111/112,** 102–104 (1982).
18. H. F. Dobele and B. Ruckle, "Concentration measurements of metastable C-atoms in a carbon arc by atomic fluorescence spectroscopy using an ArF ultraviolet laser," Plasma Phys. **24,** 1419–1428 (1982).
19. W. L. Wiese, "Line broadening," in *Plasma Diagnostic Techniques,* R. H. Huddlestone and S. L. Leonard, eds. (Academic, New York, 1965), pp. 269–299.
20. H. R. Griem, *Spectral Line Broadening by Plasmas* (Academic, New York, 1974), Chap. 3, pp. 170–211.
21. L. J. Radziemski, D. A. Cremers, and T. M. Niemczyk, "Measurement of the properties of a CO_2 laser induced air-plasma by double floating probe and spectroscopic techniques," Spectrochim. Acta **40B,** 517–525 (1985).
22. J. H. Eickmanns, W.-F. Hsieh, and R. K. Chang, "Plasma spectroscopy of H, Li and Na in plumes resulting from laser-induced droplet explosion," Appl. Opt. **26,** 3721–3725 (1987).
23. W. Lochte-Holtgreven, "Evaluation of plasma parameters," in *Plasma Diagnostics,* W. Lochte-Holtgreven, ed. (Wiley, New York, 1968), pp. 147–148 and 180–182.
24. W. L. Wiese, M. W. Smith, and B. M. Glennon, *Hydrogen through Neon,* Vol. I of Atomic Transition Probabilities, NSRDS-NBS-4 (U.S. Government Printing Office, Washington, D.C., 1966).
25. W. L. Wiese, M. W. Smith, and B. M. Miles, *Sodium through Calcium,* Vol. II of Atomic Transition Probabilities, NSRDS-NBS-22 (U.S. Government Printing Office, Washington, D.C., 1969).
26. G. Bekefi, C. Deutsch, and B. Yaakobi, "Spectroscopic diagnostics of laser plasmas," in *Principles of Laser Plasmas,* G. Bekefi, ed. (Wiley, New York, 1976), pp. 592–594.
27. H. R. Griem, "Validity of local thermal equilibrium in plasma spectroscopy," Phys. Rev. **131,** 1170–1176 (1963).
28. A. P. Thorne, *Spectrophysics* (Chapman & Hall, New York, 1988), Chap. 13, pp. 355–358.
29. J. Stricker and J. G. Parker, "Experimental investigations of electrical breakdown in nitrogen and oxygen induced by focused laser radiation at 1.064μ," J. Appl. Phys. **53,** 851–855 (1982).
30. S. V. Dresvin, *Physics and Technology of Low-Temperature Plasmas* (Iowa State U. Press, Ames, Iowa, 1977), Chap. 2, p. 24.